Modeling high frequency magnetic losses in transverse field annealed amorphous ribbons

Published paper @DOI: 10.1109/TMAG.2014.2361534

Modeling high frequency magnetic losses in transverse anisotropy amorphous ribbons

Oriano Bottauscio, Fausto Fiorillo, Cinzia Beatrice, Ambra Caprile, and Alessandro Magni

Istituto Nazionale di Ricerca Metrologica (INRIM), 10135 Torino, Italy

The superior high-frequency magnetic behavior of transverse anisotropy amorphous ribbons can be qualitatively interpreted in terms of rotation dominated magnetization process and quantitatively predicted describing the spin dynamics by the Landau-Lifshitz-Gilbert (LLG) equation in association with the electromagnetic diffusion equation. The theory is applied to comprehensive measurements performed on Co-based alloys, tested as field annealed tapewound rings from DC to 1 GHz with combination of fluxmetric and transmission line methods. The LLG equation is numerically solved considering the role of magnetostatic, exchange, anisotropy, eddy current, and applied fields. It accurately describes the high-frequency energy losses, ensuing from eddy currents and spin damping. By further considering the low-frequency domain wall contribution, a full scenario for the broadband losses is achieved.

***Index Terms*—Magnetic losses, high-frequency magnetic properties, amorphous alloys, Landau-Lifshitz-Gilbert equation**

I. Introduction

TRANSVERSE field annealed amorphous and nanocrystalline tapes display excellent broadband magnetic properties, showing, in particular, higher permeability and lower energy losses than soft ferrites at all frequencies, up to the GHz range [1-4]. This occurs in spite of their metallic character and the ensuing energy dissipation by eddy-current losses. A chief reason for the efficient soft magnetic behavior of these materials, where a mild induced transverse anisotropy (~10 ÷ ~100 J/m^3) suffices to create a defined transverse 180° domain wall (dw) structure, lies in the specific nature of the magnetization process, which is mainly accomplished by moment rotations. Kerr measurements show that some dw activity actually takes place. It has, for magnetostatic reasons, a rearrangement character, providing no net contribution to the magnetization, and becomes fully damped in the MHz range [4]. It is then concluded that on entering the radiofrequency regime, where only rotations survive, the material emulates the ideal classical limit of a structureless material with fully homogeneous magnetization process [5]. The natural approach to the broadband magnetic loss behavior is based on the statistical theory of losses, keeping in mind that on entering the MHz range two fundamental loss mechanisms concur: the classical eddy current dissipation and the energy absorption due to the excitation of the spin precessional modes. Indeed, the standard approach to the classical eddy current energy losses W_{eddy}, based on the solution of the electromagnetic diffusion equation in a medium with electrical resistivity ρ, DC magnetic permeability μ and thickness d, leads to large skin effect, but grossly underestimated the energy loss. It predicts, in particular, $W_{eddy} \propto f^{1/2}$ at high frequencies, while, as shown in the example of Fig. 1, the measured loss $W \propto f$. Remarkably, as also shown in Fig. 1, better prediction of the experimental high-frequency loss is obtained introducing the frequency dependent real part μ' of the measured initial permeability (implying negligible skin effect) in the electromagnetic diffusion equation [1].

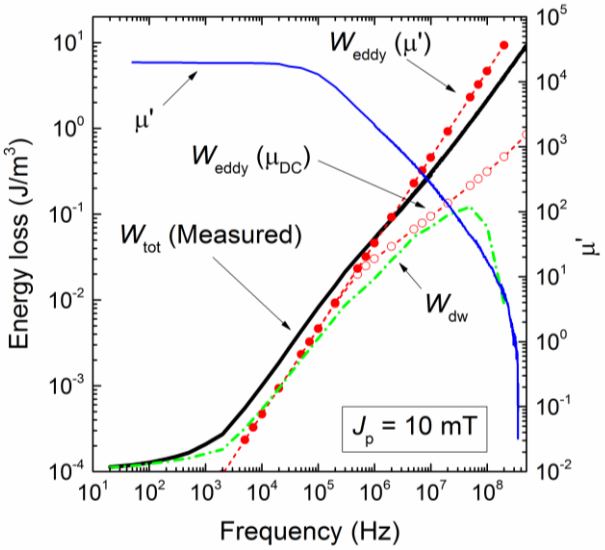

Fig. 1 - Energy loss, $W(f)$, measured in a 20 μm thick $Co_{67}Fe_4B_{14.5}Si_{14.5}$ transverse anisotropy tapewound ring sample (solid black line) and real part of the initial magnetic permeability μ'(f) (solid blue line). The symbols show the eddy current loss predicted by the Maxwell equations using either μ_{DC} (W_{eddy} (μ_{DC}), open dots) or μ'(f) (W_{eddy} (μ'), full symbols). Energy loss by dw motion (W_{dw}, dash-dot line) is negligible at high frequencies.

Given the regular antiparallel domain structure of these materials and the lack of domain wall activity at high frequencies, a simple model for the high-frequency magnetization process is envisaged, where the magnetization dynamics is described by coupled Maxwell and Landau-Lifshitz-Gilbert (LLG) equations [6-10]. This model, basically proposed in [5], is made to describe here the magnetostatic effects associated with the actual regular system of transverse bar-like domains. Simulations are compared to experiments made on different types of transverse anisotropy amorphous tapes, with thickness d ranging between 6.1 μm and 20.3 μm.

II. The Model

Based on stroboscopic Kerr observation of the domain structure of the transverse field-annealed ribbons and its

evolution with frequency, we assume that the magnetization process at high frequencies occurs as sketched in Fig. 2. The magnetization in the transverse antiparallel domains (x-axis), all having equal width w_d, oscillates around the easy axis under the action of the applied alternating field $H_a(t)$ directed along the ribbon length (y-axis). Given the symmetry of the problem, no free poles are created at the (stationary) walls. The ribbon has width w_s (x-axis), thickness d (z-axis), and length occupied by $2N + 1$ domains. The solution of the Maxwell diffusion equation in a homogenous lamination of DC permeability μ leads to the classical eddy current energy loss at given frequency f and peak polarization peak value J_p

$$W_{\text{eddy}}(f) = \frac{\pi}{2} \cdot \frac{\gamma J_p^2}{\mu} \cdot \frac{\text{sh}\gamma - \sin\gamma}{\text{ch}\gamma - \cos\gamma} \qquad [\text{J/m}^3] \qquad (1)$$

where $\gamma = \sqrt{\pi\mu d^2 f/\rho}$. We see in Fig. 1 that, because of the large skin effect predicted by (1), whose occurrence is signaled by the transition from $W_{\text{eddy}} \propto f$ to $W_{\text{eddy}} \propto f^{1/2}$, the experimental $W(f)$ is strongly underestimated. On the other hand, if the measured μ' is introduced in (1), which amounts in practice to ignore the skin effect, the dependence $W_{\text{eddy}} \propto f$ is preserved, but the experimental $W(f)$ is overestimated.

In actual fact, we are dealing with a spin system, whose collective dynamics is best described by means of the LLG equation. Let us therefore consider, exploiting the symmetry of the problem along y-axis, the magnetization $\mathbf{M}$ of a single domain, which depends only on the coordinate z. The domain is discretized along the ribbon thickness (z-axis) into F finite elements, introducing 1-D linear shape functions. In each point, $\mathbf{M}$ evolves according to the LLG equation:

$$\frac{\partial \mathbf{M}}{\partial t} = -\frac{\gamma\mu_0}{1+\alpha^2}\mathbf{M}\times\left(\mathbf{H}_{\text{eff}} + \frac{\alpha}{M_s}\mathbf{M}\times\mathbf{H}_{\text{eff}}\right), \quad |\mathbf{M}| = \mathbf{M}_s \qquad (2)$$

where $\gamma = 1.76\cdot10^{11}$ T^{-1}s^{-1} is the absolute value of the electron gyromagnetic ratio, μ_0 is the magnetic constant, α is the damping constant, $\mathbf{M}_s$ is the saturation magnetization. The effective field $\mathbf{H}_{\text{eff}}$ is the sum of the exchange $\mathbf{H}_{\text{ex}}$, magnetostatic $\mathbf{H}_{\text{ms}}$, anisotropy $\mathbf{H}_{\text{an}}$, eddy current $\mathbf{H}_{\text{eddy}}$, and applied $\mathbf{H}_a$ fields. We see here that the Maxwell diffusion equation enters the LLG equation via the eddy current field $\mathbf{H}_{\text{eddy}}$. The anisotropy field, associated with the transverse anisotropy constant $K_\perp$, is x-directed

$$H_{\text{an},x}(z) = \left(2K_\perp/\mu_0 M_s^2\right) M_x \qquad (3)$$

while the exchange field can be written as

$$\mathbf{H}_{ex}(z) = \left(2A/\mu_0 M_s^2\right)\nabla^2\mathbf{M}\,, \qquad (4)$$

where A is the stiffness constant. The magnetostatic field is expressed considering the long-range interactions among the transverse equispaced antiparallel domains, as

$$\mathbf{H}_{\text{ms}}(\mathbf{r}_0) = \frac{1}{4\pi}\sum_{n=-N}^{+N}\sum_{f=1}^{F}\int_{\partial\Omega_e}\left(\mathbf{M}(\mathbf{r}_e)\cdot\mathbf{n}_e\right)\frac{(\mathbf{r}_0-\mathbf{r}_e)}{\|\mathbf{r}_0-\mathbf{r}_e\|^3}ds \quad , \qquad (5)$$

where $\boldsymbol{r}_0$ is the source point along the z-axis (where the magnetostatic field is computed), $\boldsymbol{r}_e$ is the computational point (i.e. a point within a generic domain with magnetization $\mathbf{M}(\mathbf{r}_e)$), and $\boldsymbol{n}_e$ is the local value of the outward normal unit

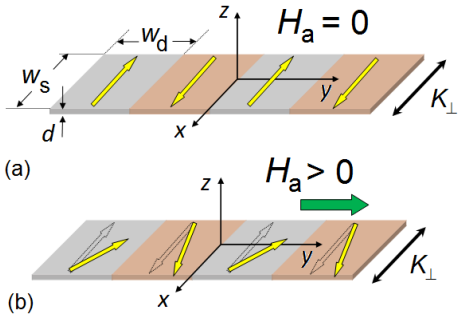

Fig. 2 – Schematic view of the magnetic domain structure of a transverse anisotropy amorphous ribbon (a) and magnetization oscillating under the effect of the field $\mathbf{H}_a$ applied along the y-axis (b).

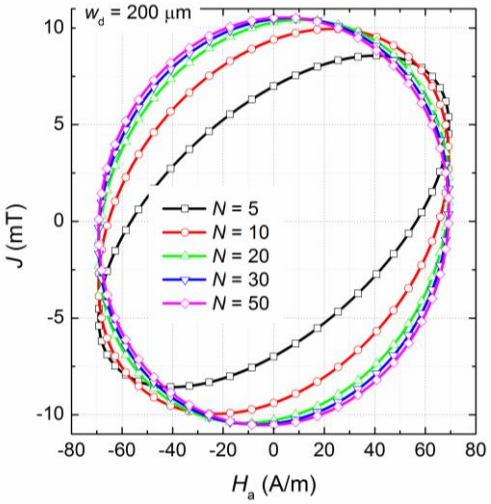

Fig. 3 – Hysteresis loops at 100 MHz in the 20 μm thick $Co_{67}Fe_4B_{15}Si_{14.5}$ ribbon calculated for increasing number N of domains and ensuing change of the domain-domain magnetostatic interaction (domain width w_d = 200 μm).

vector of the f-th element in the n-th generic domain having surface $\partial\Omega_e$. The eddy current field $\mathbf{H}_{\text{eddy}} = (0, H_{\text{eddy}}(z), 0)$ satisfies the diffusion equation

$$\frac{\partial^2 H_{\text{eddy}}}{\partial z^2} = \frac{1}{\rho}\frac{\partial B_y}{\partial t} = \frac{\mu_0}{\rho}\frac{\partial}{\partial t}\left(M_y + H_a + H_{eddy}\right) \qquad (6)$$

By solving the coupled equations (2) and (6), under the constraint $|\mathbf{M}| = M_s$ and the boundary conditions $H_{\text{eddy}}(d/2,t) = 0$ and $\partial H_{\text{eddy}}/\partial z(0,t) = 0$, the space and time evolution of $\mathbf{M}(z,t)$ in each domain is obtained. Eq. (6) is spatially discretized by the Finite Element Method. Eqs. (2) and (6) are integrated in the time domain by using a 1st order scheme (Euler scheme). To preserve the magnetization amplitude, a norm-conserving formalism, based on the Cayley transform [11], is adopted. Thus at the generic time step $\Delta t = t_{i+1} - t_i$, the magnetization is updated as

$$\mathbf{M}_{i+1} = \text{cay}(\Delta t\ \boldsymbol{\omega}_i)\mathbf{M}_i\,, \qquad (7)$$

where

$$\boldsymbol{\omega} = \frac{\gamma\mu_0}{1+\alpha^2}\left(\mathbf{H}_{\text{eff}} + \frac{\alpha}{M_s}\mathbf{M}\times\mathbf{H}_{\text{eff}}\right) \qquad (8)$$

and the cay function, applied to a generic vector $\boldsymbol{\nu} = (\nu_x, \nu_y, \nu_z)$, is defined as:

$$\mathrm{cay}(\mathbf{v}) = \left(\mathbf{I} + \mathrm{skew}[\mathbf{v}/2]\right)\left(\mathbf{I} + \mathrm{skew}[\mathbf{v}/2]\right)^{-1}, \quad (9)$$

where **I** is the identity matrix and the Lie algebra of the 3x3 skew matrices is introduced [12]

$$\mathrm{skew}[\mathbf{v}/2] = \begin{bmatrix} 0 & -v_z/2 & v_y/2 \\ v_z/2 & 0 & -v_x/2 \\ -v_y/2 & v_x/2 & 0 \end{bmatrix}. \quad (10)$$

Integration of (2) and (6) versus time is iterated until steady-state periodic conditions are reached. To account for the time scale involved in LLG equation, a time step Δt ~1 ps is adopted. This choice influences the overall computational burden, which becomes substantial in the lower frequency range (10^6 time steps in a period at the frequency f = 1 MHz).

III. Results and Discussion

Tapewound ring samples of diameter 19 mm were prepared with amorphous ribbons of composition $Co_{67}Fe_4B_{15}Si_{14.5}$ and $Co_{71}Fe_4B_{15}Si_{10}$ of width 10 mm and thickness 6.1 μm ≤ d ≤ 20 μm. They were subjected to stress relaxation by annealing at a maximum temperature of 360 °C and slow cooling with intermediate steps under transverse saturating field. By controlling the cooling sequence, a range of transverse anisotropy constants (6.5 J/m^3 ≤ $K_\perp$ ≤ 48 J/m^3), resulting in quasi-linear hysteresis loops of different slopes, was obtained. Physical parameters of the measured samples are given in Tables I and II. Energy losses for defined J_p value were measured from DC to 10 MHz by fluxmetric measurements and till 1 GHz by a transmission line method [1].

The numerical analysis of (5) shows that the magnetostatic field $\mathbf{H}_{ms}$, calculated for the range of experimental domain widths 100 μm ≤ w_d ≤ 500 μm [4] tends to asymptotically saturate with the increase of the number N of domains. Fig. 3 shows, for example, that the hysteresis loops calculated with (2) for the 20 μm thick $Co_{67}Fe_4B_{15}Si_{14.5}$ ribbons at 100 MHz does evolve with N up to about N ~ 20÷30. The adopted value N = 30 ensures a stable result. A weak effect of the domain width w_d is found. To simplify the matter, w_d = 200 μm has been assumed, according to the Kerr experiments, in all calculations. Dynamic hysteresis loops computed on the 6.1 μm and 20 μm thick $Co_{67}Fe_4B_{15}Si_{14.5}$ ribbon, at 10 MHz and 100 MHz, are compared with the experiments for J_p = 10 mT in Fig. 4. The loop area (i.e. the specific energy loss) depends on the damping constant α, here assumed equal to 0.22 for the 20 μm thick ribbon and 0.15 for the 6.1 μm thick ribbon.

TABLE I
PHYSICAL PROPERTIES OF FIELD ANNEALED $Co_{67}Fe_4B_{14.5}Si_{14.5}$

d (μm)	ρ (Ω m)	M_s (A m^{-1})	A (J m^{-1})	$K_\perp$ (J m^{-3})
6.1	141 10^{-8}	5.18 10^5	10^{-11}	9
13				7
20				8.5

TABLE II
PHYSICAL PROPERTIES OF FIELD ANNEALED $Co_{71}Fe_4B_{15}Si_{10}$

d (μm)	ρ (Ω m)	M_s (A m^{-1})	A (J m^{-1})	$K_\perp$ (J m^{-3})
17	124 10^{-8}	7.09 10^5	10^{-11}	48

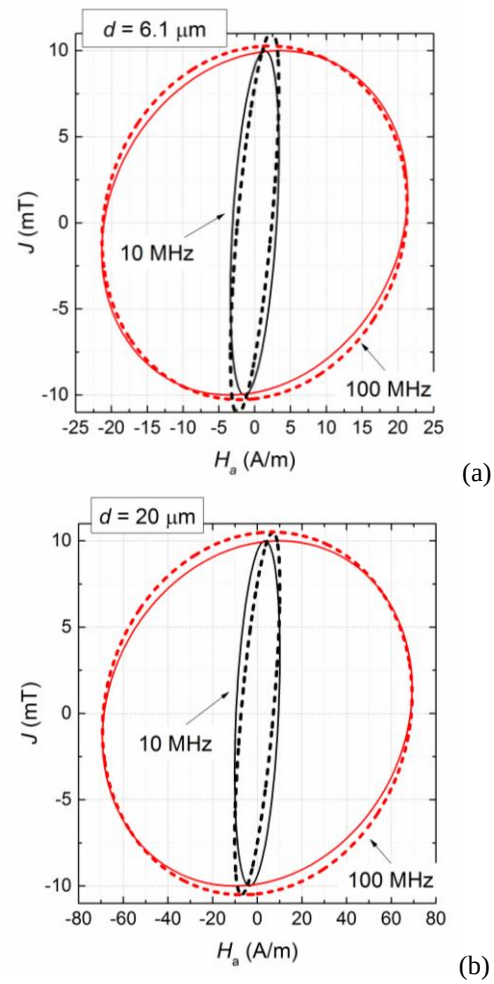

Fig. 4 – $Co_{67}Fe_4B_{15}Si_{14.5}$ ribbons: experimental (solid lines) and computed (dashed lines) dynamic hysteresis loops at 10 MHz and 100 MHz, for two sample thicknesses: 6.1 μm (a) and 20 μm (b).

These unusually large values of the LLG damping coefficient have been confirmed by pulsed inductive microwave magnetometry (PIMM) experiments, which show a dependence of α on the sample thickness [13]. A general good agreement between the energy losses measured at high frequencies and the losses calculated via (2) is found. This is illustrated by the example shown in Fig. 5, concerning $Co_{67}Fe_4B_{15}Si_{14.5}$ tapes of different thicknesses tested at J_p = 10 mT. It is found that the measured loss is shared in roughly similar proportions by the eddy current (W_{eddy}) and the spin damping (W_{sd}) mechanisms. $W(f)$ is predicted by the LLG-Maxwell model to near-linearly increase with the frequency. Thanks to the exchange mechanism, the skin effect is dramatically reduced with respect to the classical Maxwell approach, where the constitutive magnetic equation is lumped in the DC permeability (see Fig. 6). Similarly good predictive results for $W(f)$ at high frequencies are found for the $Co_{71}Fe_4B_{15}Si_{10}$ ribbon (thickness 17 μm, J_p = 5 mT), as shown in Fig. 7. Here, as in Fig. 6, the contribution by the domain wall motion $W_{dw}(f) = W_{eddy}(f) - W_{sd}(f)$ at low frequencies is apparent. It is shown in [1] that $W_{dw}(f)$ is amenable to quantitative formulation.

IV. Conclusions

The excellent high-frequency magnetic behavior of transverse anisotropy amorphous ribbons has been accurately predicted by solution of the LLG equation with nested electromagnetic diffusion equation. A relatively large value of the LLG damping constant $\alpha = 0.15 - 0.22$ is employed, consistent with recent PIMM experiments on the same materials.

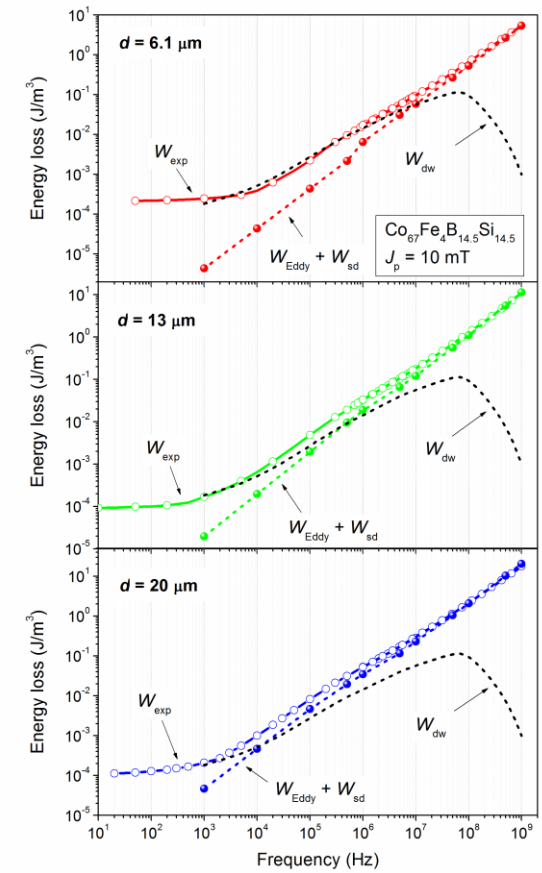

Fig. 5 – Experimental energy losses (J_p = 10 mT) up to 1 GHz in 6.1 μm, 13 μm and 20 μm thick $Co_{67}Fe_4B_{14.5}Si_{14.5}$ transverse anisotropy tapewound ring samples (open symbols) and losses calculated by coupled LLG-Maxwell equations (full symbols), including eddy currents (W_{eddy}) and spin damping mechanism (W_{sd}). The domain wall contribution (W_{dw}) is also shown.

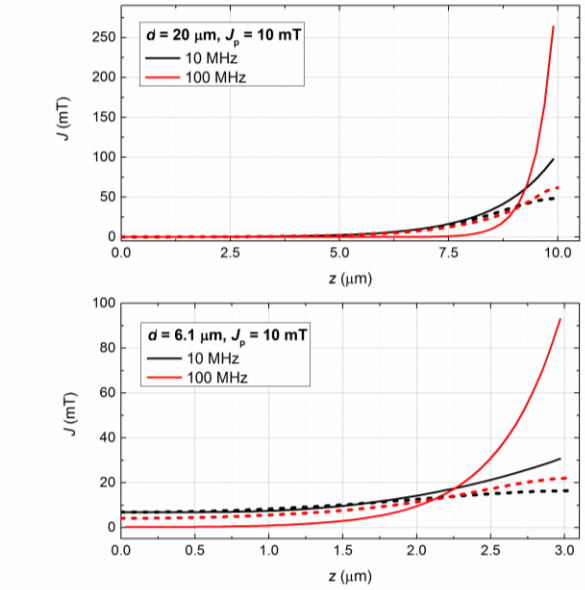

Fig. 6 –Computed magnetization profile from midplane (z = 0) to surface across the 20 μm thick (upper diagram) and 6.1 μm thick (lower diagram) $Co_{67}Fe_4B_{15}Si_{14.5}$ ribbons at 10 MHz and 100 MHz. Solid lines: classical eddy current model with μ_{DC}. Dashed lines: LLG-Maxwell approach.

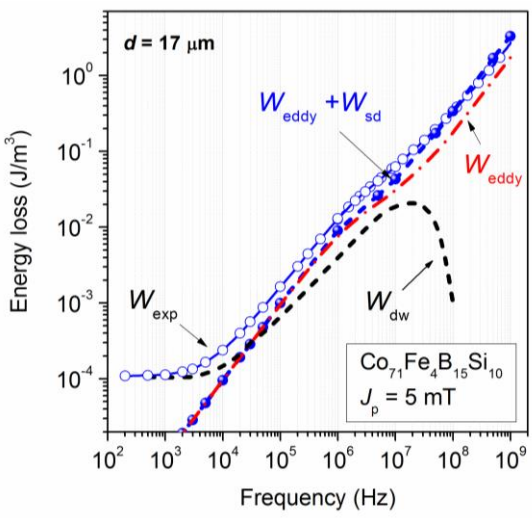

Fig. 7 – As in Fig. 5 for the 17 μm thick $Co_{71}Fe_4B_{15}Si_{10}$ transverse anisotropy ($K_\perp$ = 48 J/m³) tapewound ring sample at J_p = 5 mT. Open symbols: experiments. Full symbols: loss calculated by the LLG-Maxwell equations. The eddy current contribution (W_{eddy}) is shown by the dash-dotted line. Dashed line: contribution (W_{dw}) by the domain wall motion.

References

[1] F. Fiorillo, E. Ferrara, M. Coïsson, C. Beatrice, N. Banu, "Magnetic properties of soft ferrites and amorphous ribbons up to radiofrequencies," *J. Magn. Magn. Mater*., vol. 322, pp. 1497–1504, 2010.

[2] G. Herzer, , K. H. L. Buschow, Ed., Nanocrystalline soft magnetic alloys in Handbook of Magnetic Materials. Amsterdam, The Netherlands: Elsevier, 1997, vol. 10, 415.

[3] S. Flohrer, R. Schaefer, J. McCord, S. Roth, L. Schultz, F. Fiorillo, W. Gunther, and G. Herzer, "Dynamic magnetization process of nanocrystalline tape wound cores with transverse field-induced anisotropy", *Acta Mater*., Vol. 54, pp. 4693-4698, 2006.

[4] A. Magni, C. Beatrice, O. Bottauscio, A. Caprile, E. Ferrara, F. Fiorillo, "Magnetization process in thin laminations up to 1 GHz", *IEEE Trans. Magn.*, Vol. 48, No. 4, pp. 1363-1366, 2012.

[5] A. Magni, F. Fiorillo, E. Ferrara, A. Caprile, O. Bottauscio, C. Beatrice, "Domain wall processes, rotations, and high-frequency losses in thin laminations", *IEEE Trans. Magn*., Vol. 48, pp. 3796-3799, 2012.

[6] W.S. Ament and G.T. Rado, "Electromagnetic Effects of Spin Wave Resonance in Ferromagnetic Metals", *Phys. Rev*., Vol. 97, pp. 1558-1566, 1955.

[7] C. Serpico, I.D. Mayergoyz, and G. Bertotti, "Analysis of eddy currents with Landau-Lifshitz equations as a constitutive relation", *IEEE Trans. Magn.*, Vol. 37, pp. 3546-3549, 2001.

[8] L. Duprè, F. Olyslagerb, J. Melkebeek, "Macroscopic fields in thin ferromagnetic sheets taking into account eddy currents and Landau–Lifshitz magnetization", *J. Magn. Magn. Mater*, vol. 272–276, pp. 717–719, 2004.

[9] M. Slodicka, L. Banas, "A numerical scheme for a Maxwell–Landau–Lifshitz–Gilbert system", *Applied Mathematics and Computation*, vol. 158, pp. 79–99, 2004.

[10] K. Le, T. Tran, "A convergent finite element approximation for the quasi-static Maxwell–Landau–Lifshitz–Gilbert equations", *Computers and Mathematics with Applications*, vol. 66, pp. 1389–1402, 2013.

[11] O. Bottauscio and A. Manzin, "Efficiency of the geometric integration of Landau–Lifshitz–Gilbert equation based on Cayley transform, " *IEEE Trans. Magn.*, vol. 47, 1154-1157, 2011.

[12] D. Lewis and N. Nigam, “Geometric integration on spheres and some interesting applications,” *J. Comput., Appl. Math*., vol. 151, pp. 141–170, 2003.
[13] A. Magni, O. Bottauscio, A. Caprile, F. Celegato, E. Ferrara, and F. Fiorillo, “Spin precession by pulsed inductive magnetometry in thin amorphous plates”, *J. Appl. Phys*., Vol. 115, 17A338, 2014.